Radiomics Analysis of DTI Data to Assess Vision Outcome After Intravenous Methylprednisolone Therapy in Neuromyelitis Optic Neuritis

Yuan Tian, MD,[1,2] Zhenyu Liu, PhD,[3] Zhenchao Tang, PhD,[3,4] Mingge Li, MD,[1] Xin Lou, MD,[1] Enqing Dong, PhD,[4] Gang Liu, MD,[1] Yulin Wang, MD,[1] Yan Wang, MD,[1] Xiangbin Bian, MD,[1] Shihui Wei, MD,[5]* Jie Tian, PhD,[3,6]* and Lin Ma, MD[1]*

Background: Neuromyelitis optica-optic neuritis (NMO-ON) patients are routinely treated with intravenous methylprednisolone (IVMP). For the patients nonresponsive to IVMP, more effective but aggressive therapy of plasma exchange (PE) should be employed instead of IVMP in the first line.
Purpose: To assess the visual outcomes of NMO-ON patients after IVMP by radiomics analysis of whole brain diffusion tensor imaging (DTI) data.
Study Type: Retrospective.
Population: In all, 57 NMO-ON patients receiving IVMP therapy for 3 days.
Field Strength/Sequence: 3.0T; DTI images acquired by a single-shot echo planar image sequence; T_1 images acquired by 3D fast spoiled gradient echo (3D-FSPGR) MRI.
Assessment: In all, 200 DTI measures were extracted from the DTI data and employed as features to construct a radiomics assessment model for visual outcomes of NMO-ON patients after IVMP. The assessment performance was evaluated by area under the receiver operating characteristic curve (AUC), classification accuracy (ACC), sensitivity, specificity, and positive and negative predicted values (PPV and NPV). The selected DTI measures would reveal the white matter impairments related to visual recovery of NMO-ON patients.
Statistical Tests: The relationship between the selected DTI measures and the clinical visual characteristics were investigated by Pearson correlation, Spearman's rank correlation, and one-way analysis of variance analysis.
Results: The radiomics model obtained an ACC of 73.68% ($P = 0.002$), AUC of 0.7931, sensitivity of 0.6207, specificity of 0.8571, PPV of 0.8182, and NPV of 0.6857 in assessing visual outcomes of the NMO-ON patients after IVMP treatment. The selected DTI measures revealed white matter impairments related to the visual outcomes in the white matter tracts of vision-relevant regions, motor-related regions, and corpus callosum. The white matter impairments were found significantly correlated with the disease duration and the length of lesions in the optic nerve.
Data Conclusion: Radiomics analysis of DTI data has great potential in assessing visual outcomes of NMO-ON patients after IVMP therapy.
Level of Evidence: 2
Technical Efficacy: Stage 4

J. MAGN. RESON. IMAGING 2018.

View this article online at wileyonlinelibrary.com. DOI: 10.1002/jmri.26326

Received May 22, 2018, Accepted for publication Aug 15, 2018.

*Address reprint requests to: L.M., Department of Radiology, Chinese PLA General Hospital, Beijing, China. E-mail: cjr.malin@vip.163.com; J.T., CAS Key Laboratory of Molecular Imaging, Institute of Automation, Beijing, China. E-mail: jie.tian@ia.ac.cn; S.W., Department of Ophthalmology, Chinese PLA General Hospital, Beijing, China. E-mail: weishihui706@hotmail.com.

The first three authors contributed equally to this work.

From the [1]Department of Radiology, Chinese PLA General Hospital, Beijing, P.R. China; [2]Department of Radiology, 309th Hospital of Chinese People's Liberation Army, Beijing, P.R. China; [3]CAS Key Laboratory of Molecular Imaging, Institute of Automation, Beijing, P.R. China; [4]School of Mechanical, Electrical & Information Engineering, Shandong University, Weihai, Shandong Province, P.R. China; [5]Department of Ophthalmology, Chinese PLA General Hospital, Beijing, P.R. China; and [6]University of Chinese Academy of Sciences, Beijing, P.R. China

Additional supporting information may be found in the online version of this article.

© 2018 International Society for Magnetic Resonance in Medicine

Neuromyelitis optica (NMO) is a severe autoimmune inflammatory demyelinating disease of the central nervous system (CNS); it is often associated with an antibody targeting aquaporin-4 (AQP-4) and commonly seen in East Asia,[1] which would lead to attacks of optic neuritis (ON) and transverse myelitis.[2] Neuromyelitis optica-optic neuritis (NMO-ON) usually presents as severe visual impairment in the clinic and is frequently characterized by poor visual outcomes.[3] Furthermore, irreversible loss of vision can be caused by just two attacks of NMO-ON.[4]

Considering the high risk of visual disability, effective treatments are necessary for NMO-ON patients to prevent bad visual outcomes. Clinically, high-dose intravenous methylprednisolone (IVMP) is conventionally employed as the first-line treatment in NMO-ON[5]; nevertheless, the therapy is only clinically effective for a proportion of patients.[6] Alternatively, plasma exchange (PE) with subtraction of the agents responsible for inflammation in NMO-ON has served as an effective treatment for patients nonresponsive to IVMP.[7] Due to the relatively high risk of complications (anaphylactic reactions, myocardial infarction) and complexity of implementation, the application of PE as a first-line treatment for NMO-ON is limited in the clinic. In most situations, PE treatment is just used as a remedial therapy for the NMO-ON patients showing nonsatisfying visual recovery after IVMP treatment.[8] It is noteworthy that irreversible visual impairment might occur for the patients failing to respond to IVMP.[9] Nevertheless, the impairments could possibly have been prevented if they had received PE treatment in the first place. Timely application of PE is considered critical to acquire good visual outcomes for the patients nonresponsive to IVMP, especially in more serious cases.[10] Thus, there is an urgent need to identify the patients nonresponsive to IVMP prior to any treatment. Precise assessment of the visual outcomes of IVMP treatment in NMO-ON would aid the therapeutic decision of whether to use PE as a first-line treatment.

Previous studies have reported clinical characteristics evaluation of visual outcome,[11,12] such as the lesion length and the location of optic nerve detected by orbital magnetic resonance imaging (MRI), reduced visual evoked potential amplitude, and extent of original visual damage.[13,14] Although these studies provided an understanding of the clinical characteristics relating to visual recovery of NMO-ON, there has been no study exploring the feasibility of employing quantitative measures of medical images to assess the visual outcomes. Diffusion tensor imaging (DTI) allows noninvasive in vivo assessment of the white matter structure integrity of optic nerve tissue.[15] In addition, there are also studies showing the promising evaluation ability of DTI data for visual outcomes in ON.[16,17] Previous studies have shown that DTI data analysis enabled the identification of occult tissue damage in normal-appearing white matter (NAWM) of NMO.[18–20] It was supposed that the DTI measures revealing the white matter impairments might have the potential to assess the visual outcome of NMO-ON after IVMP.[21]

In recent years, radiomics is proposed as a promising approach to solve clinical problems by using the high-dimensional features derived from medical imaging data.[22,23] Previous studies have demonstrated that radiomics analysis achieved outstanding performance in evaluating treatment response, estimating prognosis, and aiding clinical diagnosis.[24,25] Liu et al employed radiomics analysis of MRI data to evaluate the pathological complete response to neoadjuvant chemoradiotherapy in locally advanced rectal cancer and obtained satisfying performance.[26]

In the current study, we aimed to assess the visual recovery of NMO-ON after IVMP treatment by radiomics analysis of DTI data. Furthermore, it was expected that the results might provide insight into the white matter impairments related to visual recovery in NMO-ON.

Materials and Methods

Subjects

Ethical approval was obtained for our retrospective study by the Institutional Review Board of the Chinese PLA General Hospital. This study retrospectively enrolled 57 patients clinically diagnosed as neuromyelitis optica spectrum disorder[2] in conjunction with ON between October 2014 and May 2017 (recruitment is provided in Fig. S1 of the Supplementary Material). Neuromyelitis optica spectrum disorder refers to characteristic clinical symptoms such as ON, longitudinally extensive transverse myelitis, and other core clinical manifestations (including area postrema syndrome, acute diencephalic clinical syndrome, and acute brainstem syndrome).[2] In the present study, the inclusion criteria were: 1) no other neurological history; 2) no abnormalities of the spinal cord and brain by conventional MRI; 3) unilateral ON patients; 4) late onset of ON within the 4 weeks prior to the corticosteroid treatment. Patients were excluded if they presented with optic neuropathy other than ON or had corticosteroids within the 8 weeks preceding our IVMP treatment. All the patients were recruited as outpatients or inpatients of the Chinese PLA General Hospital. All subjects underwent systematic clinical and laboratory examinations, including routine physical, neurological, and ophthalmological examinations, visual evoked potential (VEP), optical coherence tomography (OCT), and serum between aqua-porin-4 antibody (AQP4-Ab) test before IVMP treatment. Brain MRI examinations were used within 2 weeks after the IVMP treatment. All patients received methylprednisolone (1 g intravenously per day for 3 days) as a first-line treatment and were subsequently followed up for over 3 months to evaluate the visual recovery. The clinical and demographic characteristics of all the patients are provided in Table 1.

Visual acuity (VA) scoring criterion proposed by Wingerchuk et al was utilized to assess the visual recovery[27] (scoring criterion for VA is provided in Table 2). Twice VA scores were obtained respectively before the IVMP treatment and 3 months after the IVMP treatment, and the VA score increase of at least three points was regarded as a good visual outcome.[27]

TABLE 1. Demographic and Clinical Information of the Enrolled Subjects

Characteristic	Good visual outcomes (n = 29)	Poor visual outcomes (n = 28)	P-value
Age, mean ± SD	31.75 ± 12.47	35.21 ± 12.06	0.293
Gender, male/female	3/26	3/25	0.964
Disease duration, month	12.78 ± 25.97	25.53 ± 36.79	0.135
Attacks times	1.55 ± 0.69	2.07 ± 1.25	0.059
VA scores before IVMP, 1/2/3/4/5/6	0/0/0/6/16/0	0/0/0/12/16/1	0.062
VA scores after IVMP, 1/2/3/4/5/6	0/0/8/10/10/0	14/14/1/0/0/0	<0.001[a]
Lesion length, cm	1.39 ± 0.96	1.24 ± 0.89	0.540
Time from ON to IVMP	3.38 ± 2.09	4.25 ± 2.91	0.199
Lesion location, 1/2/3/4/5	18/3/2/0/6	11/5/3/1/8	0.49
AQP4-Ab status, 1:10/1:100/1:1000	5/20/4	4/18/6	0.741
OCT, RNFL before IVMP	103.13 ± 35.07	84.88 ± 29.92	0.039[a]
VEP-P100 latency, msec	130.85 ± 24.64	150.86 ± 26.85	0.005[a]
VEP-N75:P100 Amplitude, mV	10.59 ± 2.99	7.81 ± 3.43	0.002[a]

Continuous variables were presented as mean ± standard deviation. P-values were calculated by independent-samples t-tests for continuous variables, Chi-square test for gender and AQP4-Ab status, Fisher's Exact test for lesion location. The scoring criterion for VA was provided in Table S1 of the supplementary material. The lesion location was defined as: 1. orbital segment of the optic nerve; 2. canalicular segment of the optic nerve; 3. cisternal segments of the optic nerve; 4. chiasma; 5. multiple regions. The threshold for AQP4-Ab status were 1:10/1:100/1:1000. Abbreviations: VA, visual acuity; OCT, optical coherence tomography; RNFL, retinal nerve fiber layer; VEP-P100, visual evoked potential 100; SD, standard deviation.
[a]$P < 0.05$.

MRI Examinations

All MRI scans were collected on a clinical 3.0T GE Healthcare MRI scanner (Discovery750, GE Healthcare, Waukesha, WI) with a 32-channel head coil. T_1-weighted and DTI MRI scans were obtained on each participant within 2 weeks of IVMP therapy. T_1-weighted images were acquired by 3D fast spoiled gradient echo (3D-FSPGR) MRI with the following scan parameters: repetition time / echo time (TR/TE) = 8.2/ 3.2 msec, flip angle = 12°, axial acquisition with a reconstructed matrix size = 256 × 256, field of view (FOV) = 240 × 240 mm, slice thickness = 1.0 mm, contiguous spacing. DTI images were acquired by the single-shot echo planar image sequence with the following scan parameters: TR/TE = 6500/83.5 msec, flip angle = 90°, slice number = 55, one reference volume with b = 0 s/mm,^{2} 25 diffusion-weighted volumes with b = 1000 s/mm^2 and each with a unique set of gradient directions optimized for axial DTI acquisition, reconstructed matrix size = 128 × 128, slice thickness = 2 mm, FOV = 240 × 240 mm, in-plane resolution = 1.9 × 1.9 mm.^{2}

DTI Measures of Whole Brain White Matter Tracts

The pipeline for analyzing brain diffusion images (PANDA)[28] implemented based on the FMRIB Software Library (FSL)[29] were employed to obtain the DTI characteristics of white matter tracts. The DTI data were preprocessed using similar procedures to those described in previous studies[30,31]: The EddyCorrect tool was employed to correct for the head motion and eddy current distortions; the Brain Extraction tool[32] was used to remove the nonbrain tissues on the B_0 image and create the brain mask; the DTIFIT tool[33] was employed to fit a diffusion tensor at each voxel, which produced the FA, MD, AD, and RD maps after eddy current correction and brain extraction. The diffusion parameters maps including fractional anisotropy (FA), mean diffusivity (MD), axial diffusivity (AD), and radial diffusivity (RD) were derived from each subjects' DTI data after preprocessing. Second, the mean DTI measures in the 50 white matter tracts defined by the International Consortium for Brain Mapping DTI-81 (ICBM DTI-81) atlas[34] were calculated. The individual FA, MD, AD, and RD maps were registered to the FMRI58-FA template by the nonlinear registration based on the B-splines model, allowing the mean values of each white matter tract to be calculated for all the subjects. For each subject, 200 DTI measures, including FA, MD, AD, and RD were used as features in the radiomics model.

Feature Selection and Radiomics Model Construction

A logistic regression model was built to evaluate the visual outcomes of the NMO-ON patients, using the DTI measures as features:

TABLE 2. Scores of Visual Acuity

Function	Score	Description
Visual acuity	0	Normal
	1	Scotoma but VA (corrected) better than 20/30
	2	VA 20/30-20/59
	3	VA 20/60-20/199
	4	VA 20/200-20/800
	5	Count fingers only
	6	Light perception only
	7	No light perception
	8	Unknown

$$y = sigmoid\left(\sum_{j=1}^{d}\beta_j x_j + \beta_0 + \varepsilon\right) \quad (1)$$

where y was the label of the subjects (1 for good visual outcomes, 0 for poor visual outcomes), d was the number of features (200 in this case), x_i represented the DTI measures, β_i represented the model parameters, β_0 represented the constant in the logistic regression model, and ε represented the error term.

We employed the penalized approach of Elastic-net (E-net) to select the features related to the visual outcomes. The Elastic-net cost function was defined as:

$$\sum_{i=1}^{N}\left(y_i - sigmoid\left(\sum_{j=1}^{d}\beta_j x_{ij} + \beta_0\right)\right)^2 + \lambda\sum_{j=1}^{d}\left(\alpha|\beta_j| + (1-\alpha)(\beta_j)^2\right) \quad (2)$$

where y_i was the label of the i^{th} subject, N represented the number of the subject, x_{ij} was the j^{th} feature of the i^{th} subject, and λ was the regulation parameters of the model. The E-net penalty was constituted with the Lasso penalty $\sum_{j=1}^{d}|\beta_j|$ and ridge regression penalty $\sum_{j=1}^{d}(\beta_j)^2$. The Lasso penalty and ridge penalty complemented each other, achieving model sparsity while allowing the inclusion of highly correlated features.

Glmnet[35] (http://statweb.stanford.edu/~tibs/lasso.html) was employed to select the features and estimate the model parameters for the visual outcomes evaluation. The parameter α defined the weights assigned to the Lasso and ridge penalties, with α = 1 corresponding to the use of just the Lasso penalty, and α = 0 corresponding to just the ridge penalty. The λ was the regulation parameter in Lasso penalty, and was used to tune the sparsity of the model, where a large λ would lead to a sparser model. In the current study, α was chosen in the range of 0 to 1 in the step of 0.1; λ (log-scale) was chosen with the grid-mesh method, where the minimal λ was set as 0.01; and the number of λ was set as 100. The pair of α and λ achieved the best performance (area under the curve [AUC] and classification accuracy [ACC]) in the scheme of leave-one-out cross-validation (LOOCV) were chosen as the optimal parameters. The features selected by the optimal parameters were regarded as the selected features and used to construct the radiomics model. The selected features would reveal the white matter impairments associated with visual recovery.

Performance of the Radiomics Model

The performance of the radiomics model was assessed using AUC, ACC, sensitivity, specificity, positive predictive value (PPV), and negative predictive value (NPV). To estimate the significance of the classification performance, we conducted permutation tests on the classification ACC according to the framework implemented in previous studies.[36] The labels for each subject were first permuted for 500 times to provide the random dataset. Then the classification model was reconstructed for each set of permuted data and the permuted ACC values were calculated. The *P*-value for the ACC was defined as:

$$P_{ACC} = \frac{1 + N_{greaterACC}}{1 + N} \quad (3)$$

where P_{ACC} represented the *P*-values of ACC (with N being 500 here), and $N_{\text{greater ACC}}$ was the number of permutations with an ACC greater than the non-permuted ACC.

Statistical Analysis

The relationships between the white matter impairments and clinical characteristics were investigated by statistical analysis. Pearson correlation analysis was conducted between the selected DTI metrics and

the continuous clinical characteristics, including the disease duration and the lesion length. Spearman's rank correlation analysis was conducted between the selected DTI metrics and the rank variables, including the VA 3 months after IVMP treatment and AQP4-Ab status. One-way analysis of variance (ANOVA) analysis was conducted on the DTI metrics grouped by the lesion location. The significances were two-sided and the *P*-values were Bonferroni-corrected for the number of clinical characteristics (0.025 for Pearson correlation and Spearman's rank correlation; 0.05 for one-way ANOVA analysis). SPSS 18 (https://www.ibm.com/analytics/data-science/predictive-analytics/spss-statistical-software) was employed in the statistical analysis.

Results

The demographic and clinical information of the enrolled subjects is provided in Table 1. The VA scores after the IVMP treatment were significantly different between the patients with good visual outcomes and those with poor visual outcomes. No significant difference was observed in other demographic or clinical characteristics between the two patients group.

Based the features selected by the E-net penalty, the radiomics model achieved an ACC of 73.68% (P = 0.002), AUC of 0.7931, sensitivity of 0.6207, specificity of 0.8571, PPV of 0.8182, and NPV of 0.6857 under the LOOCV procedure. The ACC result was considered statistically significant, as no better permuted ACC values were observed in the permutation test (P = 0.002). The ROC plot and details of the permutation results are displayed in Fig. 1.

As revealed by the selected DTI measures, multiple white matter tracts were found to be associated with the visual recovery, including the retrolenticular part of the internal capsule (RLIC), sagittal stratum (SS), cingulum (CG), tapetum (TAP), hippocampus-cingulum region, splenium of the corpus callosum (SCC), genu of the corpus callosum (GCC), and middle cerebellar peduncle (MCP). Details on the selected white matter tracts are provided in Table 2, and 3D views are shown in Fig. 2a. The percentage contributions

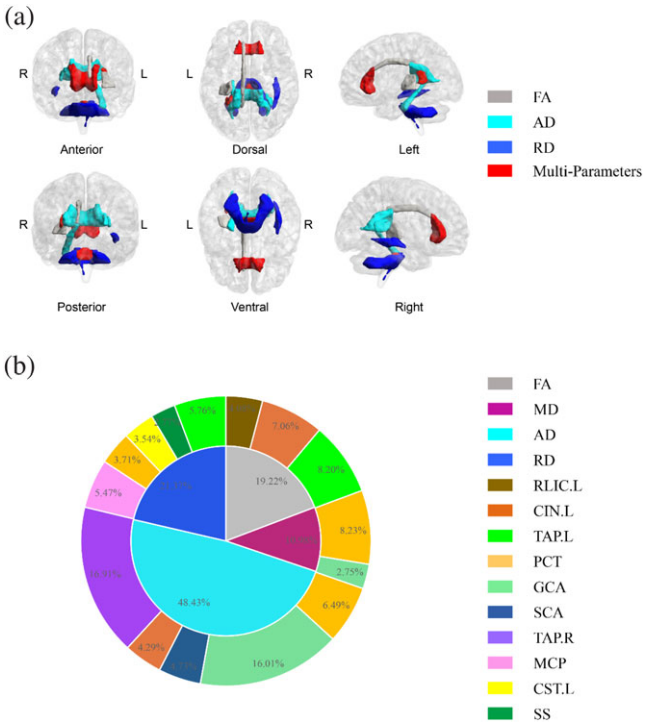

FIGURE 2: White matter tracts associated with the visual outcomes of the NMO-ON patients after intravenous methylprednisolone therapy, as identified by the Lasso regression analysis. (a) Illustration of the white matter regions identified by different DTI parameters (gray represents the tracts identified by FA, cyan represents the tracts identified by AD, blue represents the tracts identified by RD, red represents the tracts which were identified by two or more diffusion parameters). (b) Pie charts illustrating the percentage contribution of each white matter tract in predicting the visual outcomes of NMO-ON patients (the inner pie chart indicates the total contribution by FA, MD, AD, and RD; the outer pie chart indicates the contribution of each different white matter tract to the corresponding DTI parameter in the inner chart).

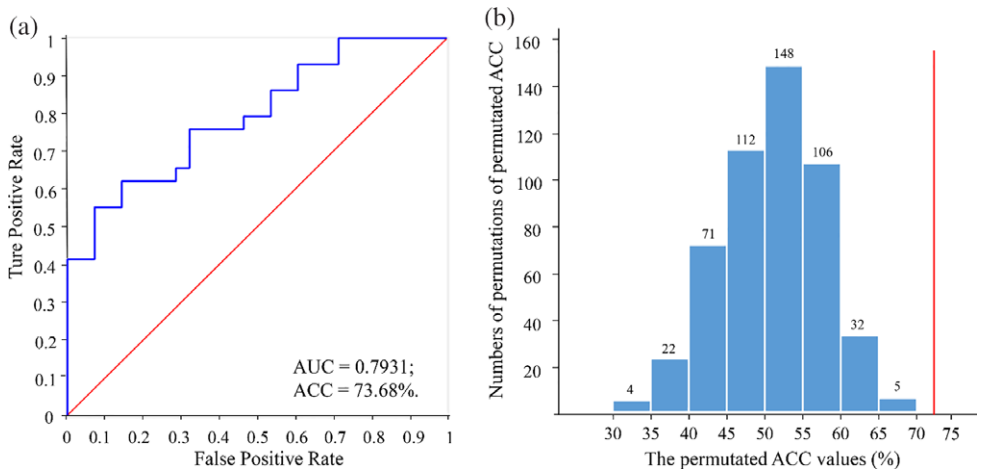

FIGURE 1: (a) ROC curve for the classification of visual outcomes in NMO-ON patients after intravenous methylprednisolone therapy (AUC = 0.7931, ACC = 73.68%). (b) The distribution of the permuted ACC values. The red line indicates the nonpermuted ACC value (73.68%). Each bar represents the number of permutations obtaining an ACC within the corresponding range. As can be seen from the illustration, no better classification ACC was observed with any of the 500 random permutations.

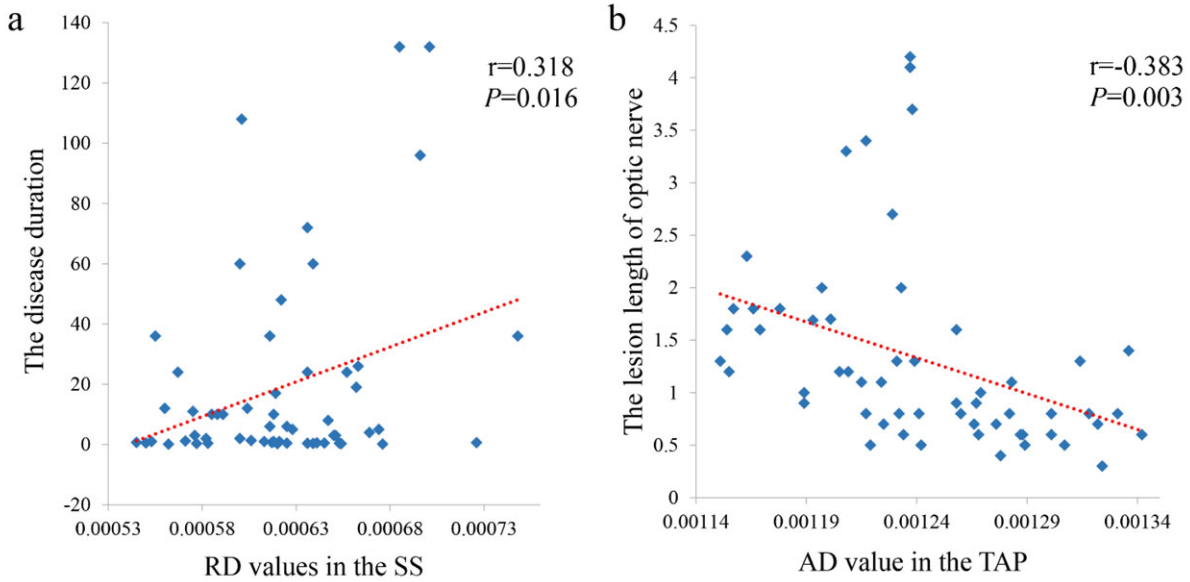

FIGURE 3: Pearson correlations between white matter DTI parameters and the clinical characteristics of NMO-ON patients. (a) RD values in the SS were significantly positively correlated with disease duration. (b) AD values in the TAP were significantly negatively correlated with optic nerve lesion length. SS, sagittal stratum; TAP, tapetum.

of the white matter tracts and DTI parameters are shown in Fig. 2b.

As indicated by Pearson correlation analysis, it was found that the disease duration was significantly positively correlated with the RD values in SS (r = 0.318; P = 0.016). The lesion length was significantly negatively correlated with the AD values in TAP (r = –0.383; P = 0.003). The Pearson correlation maps are illustrated in Fig. 3. As indicated by Spearman's rank correlation analysis, the VA after IVMP was found significantly negatively related to the FA values in TAP (rho = –0.321; P = 0.015) and AD values in SCC (rho = –0.313; P = 0.018). No significant results were found in the ANOVA analysis. The detailed statistical analysis results are provided in Table S1.

Discussion

In the current study we conducted a radiomics model based on DTI data to assess the visual outcomes of NMO-ON patients. Based on the DTI measures selected by the E-net penalty, the radiomics model could efficiently evaluate the visual outcomes of the NMO-ON patients. The selected DTI measures revealed the white matter tracts related to the visual recovery of NMO-ON, which were mainly located in the pathway of the optic radiation (OR), the corpus callosum, temporal white matter, and occipital white matter.

The present study obtained relatively moderate ACC and AUC in evaluating the visual recovery of NMO-ON patients. Due to individual variability, NMO-ON patients responded differently to IVMP treatment.[6] Nevertheless, there are still no effective clinical approaches that can accurately evaluate the visual outcomes of NMO-ON patients after IVMP treatment. Numerous studies have evaluated the visual outcomes in ON[13,14,37] without NMO. However, in contrast to isolated ON, much less research has focused on the evaluation of visual outcomes in NMO-ON.[38,39] It was found that ON lesion length in the acute phase, the impaired segment of the optic nerve, OCT data from the chronic phase, and onset age were all correlated with visual prognosis.[39] Additionally, previous studies observed an association between AQP4-Ab positivity and poor visual outcomes.[38] Although these studies provide valuable information on the neuroimaging and clinical biomarkers of visual outcomes in NMO-ON, none of these previous studies sought to implement visual prognosis at the individual level. The results of the current study indicated the potential of radiomics analysis in evaluating the visual prognosis of NMO-ON patients after IVMP.

It was noteworthy that promising specificity and PPV were obtained by the radiomics model. The specificity represented the ratio of the patient correctly classified as bad outcomes to all the patients of bad outcomes. The high specificity indicated that the patients nonresponsive to IVMP treatment could be efficiently identified. The PPV represented the ratio of the patients correctly classified as good outcomes to all the patients evaluated as good outcomes. The high PPV indicated that the patients classified as good outcomes by the radiomics model were highly possibly to be the patients who responded to IVMP treatment. Radiomics was proposed as extracting underlying pathophysiological information from medical images that were originally intended for only visual interpretation,[22] which might account for the

TABLE 3. Visual-Outcomes-Related White Matter Tracts Identified in the LASSO Regression Analysis

DTI parameters	Impaired WM tracts	Weights
FA	RLIC.L	−0.208
	CG (cingulate gyrus).L	−0.361
	TAP.L	0.419
MD	PCT (a part of MCP)	0.420
	GCC	0.140
AD	PCT (a part of MCP)	0.332
	GCC	0.818
	SCC	−0.242
	CG (hippocampus).L	0.219
	TAP.R	−0.863
RD	MCP	−0.279
	PCT (a part of MCP)	0.189
	CST.L	0.181
	SS (include ILF and IFO).R	−0.142
	TAP.L	−0.294

RLIC, retrolenticular part of the internal capsule; CG, cingulum; TAP, tapetum; PCT, Pontine crossing tract; MCP, middle cerebellar peduncle; GCC, genu of corpus callosum; SCC, splenium of corpus callosum; CST, corticospinal tracts; SS, sagittal stratum; ILF, inferior longitudinal fasciculus; IFO, inferior fronto-occipital fasciculus; R, right; L, left. The weights were obtained from the coefficients of each feature in the logistic regression model.

relatively high specificity and PPV. The promising results of our study showed the potential advantages of radiomics model in individually aiding the clinical decision of whether to use PE as the first-line treatment for NMO-ON patients.

The selected DTI measures revealed white matter changes related to the visual outcomes of NMO-ON in the vision relevant regions of the RLIC. It is known that the OR is the substantial constituent of the RLIC[34]; it begins at the lateral geniculate body, passes through the internal capsule (including the RLIC), and subsequently goes through the external SS of the temporal and occipital lobes to the striate area of the occipital cortex.[34,40] In the previous univariate analysis studies, Raz et al found obvious abnormal FA and RD values in the ORs of patients with ON,[41] and Yu et al[20] reported that increased MD and RD were found OR (included RLIC, SS) of NMO patients and MD of the OR was correlated with visual Kurtzke Functional Systems (KFS) scores. They indicated that the lesions in the optic nerves of NMO result in subsequent axonal degeneration that is the most possible pathogenesis of abnormal diffusion indexes of brain white matter. These results are consistent with our findings that features selected within the OR (including the FA value of the RLIC and the RD value of the SS) were effective in evaluating visual prognosis in NMO-ON after IVMP. Our finding provided preliminary evidence that the RD injury might be responsible for the visual outcomes after IVMP treatment of NMO-ON patients.

We also found that the white matter integrity in the corpus callosum and motor-related white matter tracts were related to the visual outcomes of NMO patients. In agreement with our findings, previous univariate analysis studies reported that white matter bunches along the corpus callosum were abnormal in NMO patients.[19,42] Bester et al demonstrated FA abnormalities in the corpus callosum of patients with ON, and Wallerian degeneration was believed to have a key role in the first stage of the disease.[43] MD and AD values in the corpus callosum were also found related to visual recovery in the present study. We supposed that the corpus callosum was the crucial interhemispheric structure of the whole white matter, so it was therefore most vulnerable to the degeneration or damage brought about by NMO-ON. The crucial white matter tracts identified in the current study also involved motor-related white matter tracts, including the corticospinal tract (CST) and MCP, which

agrees with the finding of abnormal CST in NMO by previous studies.[19,20] Yu et al[20] also found close correlations between diffusion indexes of the CST and the lesion of the spinal cord. Although the spinal cord of the NMO patients in our study were normal with MRI, occult damage could not be ruled out.

In the correlation analysis, we found that disease duration correlated with the RD value in the SS. It might be inferred that longer disease duration might be indicative of more serious injury of white matter tracts. It was also found that the length of lesions in the optic nerve correlated with AD values in the right TAP. This agreed with the previous finding that the AD value was decreased in the longer lesion of ON,[44] and that the AD value in acute ON was associated with a worse visual outcome.[15] In addition, the higher VA scores was found significantly correlated with the white matter impairments in GCC and TAP, which indicated that the more worse visual ability was related to the worse white matter integrity in the regions of the corpus callosum.[18]

There were still several limitations in the current study. First, the sample size of the current study was relatively small due to the rarity of the disease. Thus, we employed the scheme of LOOCV instead of independent validation to assess the performance of the radiomics model. Future study with larger numbers of patients and more diversified data is needed to confirm and further explore the findings of the current study in independent validation. Second, NMO-ON patients with negative AQP-4 Ab were not enrolled in the current study. Although negative AQP-4 Ab was rather rare in NMO-ON patients, the inclusion of this cohort would provide more insight into the evaluation of visual outcomes of NMO-ON after IVMP treatment. Further studies including negative AQP-4 Ab should be conducted in the future.

In conclusion, our study indicated the great potential of the radiomics analysis of brain DTI data in assessing the visual outcome of NMO-ON, which might help to aid the therapeutic decision of whether to use PE in the first line. In addition, our results demonstrated that the white matter impairments in vision-related regions, motor-related regions, and the CC might account for the poor visual prognosis of NMO-ON patients.

Acknowledgment

Contract grant sponsor: National Key Research and Development Plan of China; Contract grant numbers: 2017YFA0205200 and 2016YFC0103001; Contract grant sponsor: National Natural Science Foundation of China; Contract grant numbers: 81227901, 81501549, 81527805, and 81772012; Contract grant sponsor: Beijing Municipal Science & Technology Commission; Contract grant numbers: Z171100000117023, Z161100002616022; Contract grant sponsor: 309th Hospital of Chinese People's Liberation Army; Contract grant number: 2014ZD-003.

We thank Karl Embleton, PhD, from Liwen Bianji, Edanz Group China (www.liwenbianji.cn/ac), for editing the English text of a draft of the article.

References

1. Kira J. Neuromyelitis optica and opticospinal multiple sclerosis: Mechanisms and pathogenesis. Pathophysiology 2011;18:69–79.
2. Wingerchuk DM, Banwell B, Bennett JL, et al. International consensus diagnostic criteria for neuromyelitis optica spectrum disorders. Neurology 2015;85:177–189.
3. Merle H, Olindo S, Jeannin S, et al. Treatment of optic neuritis by plasma exchange (add-on) in neuromyelitis optica. Arch Ophthalmol 2012;130: 858–862.
4. Merle H, Olindo S, Bonnan M, et al. Natural history of the visual impairment of relapsing neuromyelitis optica. Ophthalmology 2007;114: 810–815.
5. Palace J, Leite MI, Jacob A. A practical guide to the treatment of neuromyelitis optica. Pract Neurol 2012;12:209–214.
6. Hickman SJ, Dalton CM, Miller DH, Plant GT. Management of acute optic neuritis. Lancet 2002;360:1953–1962.
7. Vincent A. Autoimmune channelopathies: well-established and emerging immunotherapy-responsive diseases of the peripheral and central nervous systems. J Clin Immunol 2010;30(Suppl 1):S97–102.
8. Biswas A, Mukherjee A. Therapy of NMO spectrum disorders. Ann Indian Acad Neurol 2015;18(Suppl 1):S16–23.
9. Toosy AT, Mason DF, Miller DH. Optic neuritis. Lancet Neurol 2014;13: 83–99.
10. Bonnan M, Cabre P. Plasma exchange in severe attacks of neuromyelitis optica. Mult Scler Int 2012;2012:787630.
11. Klistorner A, Graham S, Fraser C, et al. Electrophysiological evidence for heterogeneity of lesions in optic neuritis. Invest Ophthalmol Visual Sci 2007;48:4549–4556.
12. Trip SA, Schlottmann PG, Jones SJ, et al. Retinal nerve fiber layer axonal loss and visual dysfunction in optic neuritis. Ann Neurol 2005;58: 383–391.
13. Hickman SJ, Toosy AT, Miszkiel KA, et al. Visual recovery following acute optic neuritis—a clinical, electrophysiological and magnetic resonance imaging study. J Neurol 2004;251:996–1005.
14. Dunker S, Wiegand W. Prognostic value of magnetic resonance imaging in monosymptomatic optic neuritis. Ophthalmology 1996;103: 1768–1773.
15. Naismith RT, Xu J, Tutlam NT, et al. Diffusion tensor imaging in acute optic neuropathies: predictor of clinical outcomes. Arch Neurol 2012;69: 65–71.
16. Naismith RT, Xu J, Tutlam NT, et al. Disability in optic neuritis correlates with diffusion tensor-derived directional diffusivities. Neurology 2009;72: 589–594.
17. Naismith RT, Xu J, Tutlam NT, Trinkaus K, Cross AH, Song SK. Radial diffusivity in remote optic neuritis discriminates visual outcomes. Neurology 2010;74:1702–1710.
18. Zhao DD, Zhou HY, Wu QZ, et al. Diffusion tensor imaging characterization of occult brain damage in relapsing neuromyelitis optica using 3.0T magnetic resonance imaging techniques. NeuroImage 2012;59:3173–3177.
19. Liu Y, Duan Y, He Y, et al. A tract-based diffusion study of cerebral white matter in neuromyelitis optica reveals widespread pathological alterations. Mult Scler 2012;18:1013–1021.
20. Yu C, Lin F, Li K, et al. Pathogenesis of normal-appearing white matter damage in neuromyelitis optica: diffusion-tensor MR imaging. Radiology 2008;246:222–228.

21. Ciccarelli O, Toosy AT, Hickman SJ, et al. Optic radiation changes after optic neuritis detected by tractography-based group mapping. Hum Brain Mapp 2005;25:308–316.

22. Lambin P, Rios-Velazquez E, Leijenaar R, et al. Radiomics: extracting more information from medical images using advanced feature analysis. Eur J Cancer 2012;48:441–446.

23. Liu Z, Wang Y, Liu X, et al. Radiomics analysis allows for precise prediction of epilepsy in patients with low-grade gliomas. Neuroimage Clin 2018;19:271–278.

24. Gevaert O, Xu J, Hoang CD, et al. Non-small cell lung cancer: identifying prognostic imaging biomarkers by leveraging public gene expression microarray data—methods and preliminary results. Radiology 2012;264: 387–396.

25. Guo J, Liu Z, Shen C, et al. MR-based radiomics signature in differentiating ocular adnexal lymphoma from idiopathic orbital inflammation. Eur Radiol 2018 [Epub ahead of print].

26. Liu Z, Zhang XY, Shi YJ, et al. Radiomics analysis for evaluation of pathological complete response to neoadjuvant chemoradiotherapy in locally advanced rectal cancer. Clin Cancer Res 2017;23: 7253–7262.

27. Wingerchuk DM, Hogancamp WF, O'Brien PC, Weinshenker BG. The clinical course of neuromyelitis optica (Devic's syndrome). Neurology 1999;53:1107–1114.

28. Cui Z, Zhong S, Xu P, He Y, Gong G. PANDA: a pipeline toolbox for analyzing brain diffusion images. Front Hum Neurosci 2013;7:42.

29. Smith SM, Jenkinson M, Woolrich MW, et al. Advances in functional and structural MR image analysis and implementation as FSL. NeuroImage 2004;23(Suppl 1):S208–219.

30. Tang Z, Liu Z, Li R, et al. Identifying the white matter impairments among ART-naive HIV patients: a multivariate pattern analysis of DTI data. Eur Radiol 2017 [Epub ahead of print].

31. Wang B, Liu Z, Liu J, Tang Z, Li H, Tian J. Gray and white matter alterations in early HIV-infected patients: Combined voxel-based morphometry and tract-based spatial statistics. J Magn Reson Imaging 2016;43: 1474–1483.

32. Smith SM. Fast robust automated brain extraction. Hum Brain Mapp 2002;17:143–155.

33. Basser PJ, Mattiello J, LeBihan D. MR diffusion tensor spectroscopy and imaging. Biophys J 1994;66:259–267.

34. Mori S, Oishi K, Jiang H, et al. Stereotaxic white matter atlas based on diffusion tensor imaging in an ICBM template. NeuroImage 2008;40: 570–582.

35. Friedman J, Hastie T, Tibshirani R. Regularization paths for generalized linear models via coordinate descent. J Stat Softw 2010;33:1–22.

36. Ojala M, Garriga GC. Permutation tests for studying classifier performance. J Mach Learn Res 2010;11:1833–1863.

37. Miller DH, Newton MR, van der Poel JC, et al. Magnetic resonance imaging of the optic nerve in optic neuritis. Neurology 1988;38:175–179.

38. Piccolo L, Woodhall M, Tackley G, et al. Isolated new onset 'atypical' optic neuritis in the NMO clinic: serum antibodies, prognoses and diagnoses at follow-up. J Neurol 2016;263:370–379.

39. Akaishi T, Nakashima I, Takeshita T, et al. Lesion length of optic neuritis impacts visual prognosis in neuromyelitis optica. J Neuroimmunol 2016; 293:28–33.

40. Kitajima M, Korogi Y, Takahashi M, Eto K. MR signal intensity of the optic radiation. AJNR Am J Neuroradiol 1996;17:1379–1383.

41. Raz N, Bick AS, Ben-Hur T, Levin N. Focal demyelinative damage and neighboring white matter integrity: an optic neuritis study. Mult Scler 2015;21:562–571.

42. Chan KH, Tse CT, Chung CP, et al. Brain involvement in neuromyelitis optica spectrum disorders. Arch Neurol 2011;68:1432–1439.

43. Bester M, Heesen C, Schippling S, et al. Early anisotropy changes in the corpus callosum of patients with optic neuritis. Neuroradiology 2008;50: 549–557.

44. van der Walt A, Kolbe SC, Wang YE, et al. Optic nerve diffusion tensor imaging after acute optic neuritis predicts axonal and visual outcomes. PLoS One 2013;8:e83825.